Modeling the particle flux effect on distribution of ^{230}Th in the equatorial Pacific

Mark Siddall,[1] Robert F. Anderson,[1] Gisela Winckler,[1] Gideon M. Henderson,[2]
Louisa I. Bradtmiller,[1] David McGee,[1] Allison Franzese,[1] Thomas F. Stocker,[3]
and Simon A. Müller[3,4]

[1] The normalization of sediment accumulation rates by ^{230}Th is increasingly used to constrain particle rain rates because ^{230}Th is produced at a known rate in the water column and removed relatively quickly to the sediment. Several recent contributions have questioned this approach and suggested that the preferential removal of ^{230}Th in areas of high particle flux, the "particle flux effect," introduces a systematic bias in the ^{230}Th normalization technique. We use a circulation model that includes a description of particle scavenging to show that the particle flux effect cannot explain observations of high ^{230}Th accumulation in equatorial Pacific sediments (relative to ^{230}Th production in the water column). We further consider the possible variation of particle rain rates over time. We find only a minimal sensitivity in the particle flux effect due to increases in the particle rain rate at the equatorial Pacific by a factor of up to 10. This situation exists because the residence time of ^{230}Th in the water column is too short to permit significant lateral transport with reasonable isopycnal mixing coefficients. We conclude that the increased rates of ^{230}Th accumulation found in equatorial Pacific sediments deposited during the Last Glacial Maximum cannot have been caused by the particle flux effect.

1. Introduction

[2] Production of ^{230}Th in the ocean occurs by the α decay of ^{234}U. The activity of U in the ocean is very nearly uniform [*Chen et al.*, 1986] so that ^{230}Th is effectively produced at a constant rate throughout the ocean. The short residence time of ^{230}Th in the water column (10–30 years [*Anderson et al.*, 1983]) inspired the development of the ^{230}Th normalization technique [*Bacon*, 1984]. This method is based on the assumption that the rapid scavenging of ^{230}Th produced in the water column [*Bacon and Anderson*, 1982; *Nozaki et al.*, 1987] results in the flux of ^{230}Th to the seafloor always being close to its rate of production. If this assumption is correct, scavenged ^{230}Th can be used as a reference to estimate the settling flux of other sedimentary constituents and to correct for sediment redistribution on the seafloor [*Henderson and Anderson*, 2003; *Francois et al.*, 2004]. Assuming no complicating effects the ratio of ^{230}Th accumulation in the sediment to its rate of production in the overlying water column (the "focusing factor") would be 1. However, this ratio often deviates from 1, indicating that

^{230}Th is removed from some areas and added to others. The cause of this redistribution is the root of the controversy detailed below.

[3] Alongside ^{230}Th normalization, mass accumulation rates (MAR) based on age models are also commonly used to estimate changes in particle rain rate from the surface. Such age models are often based on down-core ^{14}C dating or δ^{18}O stratigraphy. Age-model-based accumulation rates are calculated as the product of constant sedimentation rates between dated horizons and sediment dry bulk densities. This approach does not allow for the redistribution of sediments on the seafloor by bottom currents. Consequently, sediment accumulation may not necessarily reflect the true vertical rain rate (particle flux) originating from the overlying water column. Age-model-based MAR calculation and ^{230}Th normalization sometimes give very different results. Such disagreements have been widely documented in the equatorial Pacific, where age-model-based MARs often indicate higher fluxes during the last glacial period [*Lyle et al.*, 2002], while ^{230}Th normalization suggests unchanged or even lower glacial fluxes [*Marcantonio et al.*, 2001; *Loubere et al.*, 2004].

[4] There has been a good deal of controversy between these two approaches: the proponents of ^{230}Th normalization argue that differences between ^{230}Th-based and age-model-based MARs simply reflect changes in sediment focusing or age model errors, and that age-model-based MARs often do not accurately record variations in vertical flux from the overlying water (see *Francois et al.* [2007] for discussion). The opponents of ^{230}Th normalization argue

[1]Lamont-Doherty Earth Observatory of Columbia University, Palisades, New York, USA.
[2]Department of Earth Sciences, Oxford University, Oxford, UK.
[3]Climate and Environmental Physics, Physics Institute, University of Bern, Bern, Switzerland.
[4]Now at Department of Earth and Environmental Sciences, Open University, Milton Keynes, UK.

Table 1. Focusing Factors (Ψ) in the Global Ocean as Derived From Equation (2) and the Data From Table S1 in Auxiliary Material[a]

Core	Latitude, deg	Longitude, deg	Depth, m	$\Psi_{Holocene}$	$\Psi_{Glacial}$	Ψ_{Gl}/Ψ_{Hol}	Reference
TT013 MC112	5.00N	140.00W	4560	1	-	-	*Berelson et al.* [1997]
TT013 MC34	5.00S	140.00W	4391	1.1	-	-	*Berelson et al.* [1997]
TT013 MC27	3.00S	140.00W		1.1	-	-	*Berelson et al.* [1997]
TT013 MC97	2.00N	140.00W	4540	1.1	-	-	*Berelson et al.* [1997]
TT013 MC69	0.00N	140.00W	4440	1.9	-	-	*Berelson et al.* [1997]
TT013 MC19	2.00S	140.00W	4475	1.9	-	-	*Berelson et al.* [1997]
MANOP B25	1.05N	139.02W	4401	0.7	0.8	1.1	*Marcantonio et al.* [2001]
TT013-PC18	2.00S	139.00W	4354	2.8	0.7	0.3	*Marcantonio et al.* [1996]
TT013-PC72	0.00N	139.00W	4298	2.3	2.3	1	*Marcantonio et al.* [1995]
MANOP B18	1.06N	138.80W	4281	0.9	0.6	0.7	*Marcantonio et al.* [2001]
61 BX1	0.91N	140.04W	4328	1.4	1.9	1.4	*Yang et al.* [1990]
54 BX1	1.01N	133.70W	4212	1.5	2	1.3	*Yang et al.* [1990]
53 BX1	0.98N	124.63W	4516	1.8	3	1.7	*Yang et al.* [1990]
52 BX1	1.01N	118.20W	3857	1.2	1.8	1.5	*Yang et al.* [1990]
ODP-849B	0.18N	110.52W	3851	2.1	3	1.4	*Pichat et al.* [2004]
50 BX1	1.03N	104.41W	3473	1.8	2.3	1.3	*Yang et al.* [1990].
RC13-110	0.10N	95.65W	3231	2	1.6	0.8	*Loubere et al.* [2004]
ODP-846B	3.10S	90.82W	3307	2.1	3.7	1.8	*Loubere et al.* [2004]
ME0005-24JC	0.02N	86.46W	2941	4.9	5.5	1.1	*Kienast et al.* [2007]
Y69-71	0.10N	86.48W	2740	2.5	3.6	1.4	*Kienast et al.* [2007]
P7	2.60N	83.79W	3085	1.2	1.9	1.6	*Kienast et al.* [2007]
Y71-6-12	16.45N	77.57W	2734	1.4	0.9	0.6	*S. S. Kienast et al.* (2007)[b]
ME0005-27JC	1.85S	82.79W	2203	1.8	1.7	0.9	*Kienast et al.* [2007]
VNT01-8PC	0.03N	110.48W	3791	1.6	2.3	1.4	*S. S. Kienast et al.* (2007)[b]
TR163-19	2.26N	90.95W	2348	2.2	2.5	1.1	*Kienast et al.* [2007]
TR163-31	3.60S	83.95W	3209	1.6	3.4	2.1	*Kienast et al.* [2007]
V19-28	2.37S	84.65W	2720	2	3.5	1.8	*Lao et al.* [1992]
V19-29	3.58S	83.93W	3157	2.4	2.4	1	*Lao et al.* [1992]
KLH 093	1.50N	102.06W	3260	2.1	2.5	1.2	*Frank et al.* [1994]
KLH 068	1.23N	101.61W	2870	1.3	1.6	1.2	*Frank et al.* [1994]
GeoB2124-1	20.96S	39.56W	2003	0.8	-	-	*Mollenhauer et al.* [2006]
GeoB2116-2	25.51S	36W	4164	1.7	-	-	*Mollenhauer et al.* [2006]
GeoB2826-1	31.9S	40.97W	3949	0.9	-	-	*Mollenhauer et al.* [2006]
GeoB2824-1	33.5S	42.5W	4512	0.9	-	-	*Mollenhauer et al.* [2006]
GeoB2804-2	37.54S	53.54W	1836	3	-	-	*Mollenhauer et al.* [2006]
GeoB2734-3	37.61S	53.44W	2743	1.4	-	-	*Mollenhauer et al.* [2006]
GeoB2805-1	39.29S	54.34W	2295	2.1	-	-	*Mollenhauer et al.* [2006]
GeoB2728-1	43.99S	56.97W	4643	1.4	-	-	*Mollenhauer et al.* [2006]
GeoB6339-1	45.15S	58.38W	2492	3.2	-	-	*Mollenhauer et al.* [2006]
ODP848	2.99S	110.48W	3853	1.2[c]	-	-	*McGee et al.* [2007]
ODP850	1.30N	110.52W	3786	1.25[c]	-	-	*McGee et al.* [2007]
ODP851	2.77N	110.57W	3760	1.19[c]	-	-	*McGee et al.* [2007]
ODP852	5.29N	110.08W	3860	1.28[c]	-	-	*McGee et al.* [2007]
ODP853	7.21N	109.76W	3714	0.88[c]	-	-	*McGee et al.* [2007]
RC11-77	53.05S	16.45W	4098	4.78	0.39	0.08	*Franzese et al.* [2006]
RC11-80	46.75S	0.05W	3656	2.36	1.99	0.84	*Franzese et al.* [2006]
RC11-86	35.78S	18.45E	2829	0.68	1.11	1.62	*Franzese et al.* [2006]
RC12-289	47.90S	23.70W	4484	1.61	0.71	0.44	*Franzese et al.* [2006]
RC13-227	21.88S	8.87E	4301	2.2	1.75	0.8	*Franzese et al.* [2006]
RC13-229	25.50S	11.30E	4191	1.72	4.28	2.48	*Franzese et al.* [2006]
RC13-243	36.90S	0.33E	4790	2.33	1.76	0.76	*Franzese et al.* [2006]
RC13-251	42.52S	11.67E	4341	0.93	0.45	0.48	*Franzese et al.* [2006]
RC13-255	50.58S	2.90E	3332	1.4	4.64	3.31	*Franzese et al.* [2006]
RC17-69	31.50S	32.60E	3380	1.11	0.41	0.37	*Franzese et al.* [2006]
VM14-77	29.63S	32.87E	1818	0.47	0.76	1.63	*Franzese et al.* [2006]
VM19-214	23.37S	38.85E	3092	0.72	0.61	0.85	*Franzese et al.* [2006]
VM19-240	30.58S	13.28E	3103	5.9	1.75	0.3	*Franzese et al.* [2006]
RC13-254	48.57S	5.13E	3636	2.9	1.44	0.5	*Kumar* [1994]
RC13-259	53.88S	4.93W	2677	1.73	1.16	0.67	*Kumar* [1994]
RC13-271	51.98S	4.52E	3634	13.07	7.59	0.58	*Kumar* [1994]
RC15-93	46.10S	13.23W	2714	8.14	1.98	0.24	*Kumar* [1994]
RC15-94	42.98S	20.85W	3762	3.77	1.77	0.47	*Kumar* [1994]
V22-108	43.18S	3.25W	4171	3.43	3.08	0.9	*Kumar* [1994]
RC13-140	2.867N	87.75W	2246	2.86	3.91	1.37	*L. I. Bradtmiller et al.* (2006)[b]
V19-30	3.383S	83.517W	3091	1.4	2.83	2.02	*L. I. Bradtmiller et al.* (2006)[b]
V21-40	5.517S	106.767W	3182	4.91	4.26	0.87	*L. I. Bradtmiller et al.* (2006)[b]
RC11-238	1.517S	85.817W	2573	3.79	2.51	0.66	*L. I. Bradtmiller et al.* (2006)[b]
RC13-114	1.65S	103.63W	3436	4.1	2.7	0.66	*L. I. Bradtmiller et al.* (2006)[b]
V28-203	0.95N	179.4167W	3243	1.1	0.94	0.85	*L. I. Bradtmiller et al.* (2006)[b]
RC17-177	1.45N	159.45W	2600	0.91	2.06	2.26	*L. I. Bradtmiller et al.* (2006)[b]

Table 1. (continued)

Core	Latitude, deg	Longitude, deg	Depth, m	$\Psi_{Holocene}$	$\Psi_{Glacial}$	Ψ_{Gl}/Ψ_{Hol}	Reference
MD97-2138	1.25S	146.24E	1900	3.23	3.67	1.13	L. I. Bradtmiller et al. (2006)[b]
MW91-9 BC51	0	161E	3400	1.35	2.2	1.63	L. I. Bradtmiller et al. (2006)[b]
RC16-66	0.75N	36.617W	4424	1.29	2.42	1.88	L. I. Bradtmiller et al. (2006)[b]
RC24-01	0.55N	13.65W	3837	1.06	1.9	1.79	L. I. Bradtmiller et al. (2006)[b]
RC24-07	1.333S	11.917W	3899	2.75	2.33	0.85	L. I. Bradtmiller et al. (2006)[b]
RC24-12	3.01S	11.417W	3486	3.41	2.64	0.77	L. I. Bradtmiller et al. (2006)[b]
V22-182	0.53S	17.27W	3614	2.07	1.72	0.83	L. I. Bradtmiller et al. (2006)[b]
V30-40	0.2S	23.15W	3706	1.5	1.8	1.19	L. I. Bradtmiller et al. (2006)[b]
RC13-189	1.87N	30W	3233	1.91	1.61	0.84	L. I. Bradtmiller et al. (2006)[b]
RC14-31	9S	90E	3900	1.9	-	-	L. I. Bradtmiller et al. (2006)[b]
RC08-19	24.29S	14.70W	3640	2.24	2.4	1.07	A. M. Franzese et al. (2008)[b]
RC12-291	42.60S	17.90W	3930	none	1.28	-	A. M. Franzese et al. (2008)[b]
RC12-292	39.70S	15.50W	3540	1.52	0.73	0.48	A. M. Franzese et al. (2008)[b]
RC13-188	1.82N	33.68W	3450	1.44	1.04	0.72	A. M. Franzese et al. (2008)[b]
RC13-189	1.87N	30.00W	3233	1.79	2.16	1.21	A. M. Franzese et al. (2008)[b]
RC13-263	53.80S	8.22W	3389	-	2.83	-	A. M. Franzese et al. (2008)[b]
RC13-267	55.58N	2.25E	3160	1.24	0.29	0.24	A. M. Franzese et al. (2008)[b]
RC16-77	12.65S	13.43W	3404	-	2.31	-	A. M. Franzese et al. (2008)[b]
RC24-1	0.55N	13.65W	3837	1.54	3.63	2.36	A. M. Franzese et al. (2008)[b]
RC24-7	1.33S	11.92W	3899	4.11	4.01	0.98	A. M. Franzese et al. (2008)[b]
RC24-10	2.18S	11.25W	3450	1.57	5.46	3.48	A. M. Franzese et al. (2008)[b]
RC24-16	5.03S	10.18W	3559	-	4.06	-	A. M. Franzese et al. (2008)[b]
RC24-27	5.42S	0.37W	3806	3.3	1.74	0.53	A. M. Franzese et al. (2008)[b]
V9-19	11.4S	14.3W	3349	none	-	-	A. M. Franzese et al. (2008)[b]
V10-93	24.2N	47.5W	3574	none	-	-	A. M. Franzese et al. (2008)[b]
V15-168	0.20N	39.90W	4219	-	2.39	-	A. M. Franzese et al. (2008)[b]
V22-175	8.77S	14.28W	2950	2	1.62	0.81	A. M. Franzese et al. (2008)[b]
V22-177	7.75S	14.60W	3290	-	2.94	-	A. M. Franzese et al. (2008)[b]
V22-182	0.53S	17.27W	3614	2.09	1.65	0.79	A. M. Franzese et al. (2008)[b]
V22-26	8.70N	41.30W	3720	0.87	0.98	1.13	A. M. Franzese et al. (2008)[b]
V23-112	17.3N	46.8W	2850	none	-	-	A. M. Franzese et al. (2008)[b]
V24-231	34.0S	13.8W	3438	none	-	-	A. M. Franzese et al. (2008)[b]
V25-59	1.37N	33.48W	3824	1.88	3.7	1.97	A. M. Franzese et al. (2008)[b]
V25-60	3.28N	34.83W	3749	1.88	0.49	0.26	A. M. Franzese et al. (2008)[b]
V26-17	29.90N	45.10W	3620	1.71	1.25	0.73	A. M. Franzese et al. (2008)[b]
V26-70	30.9S	17.9W	3933	none	none	-	A. M. Franzese et al. (2008)[b]
V28-89	44.53N	32.58W	3643	0.06	0.34	5.68	A. M. Franzese et al. (2008)[b]
V30-36	5.35N	27.32W	4245	0.91	0.3	0.32	A. M. Franzese et al. (2008)[b]
V30-40	0.20S	23.15W	3706	1.03	1.51	1.47	A. M. Franzese et al. (2008)[b]
V30-94	35.50N	37.80W	3680	1.8	0.35	0.2	A. M. Franzese et al. (2008)[b]
V30-96A	39.95N	33.13W	3188	1.15	2.13	1.85	A. M. Franzese et al. (2008)[b]
V34-157	41.95S	26.42E	3636	1.48	1.25	0.85	A. M. Franzese et al. (2008)[b]

[a]Values in bold are after the published data sets from *Kienast et al.* [2007], *Mollenhauer et al.* [2006], *Franzese et al.* [2006] and *McGee et al.* [2007], other values are based on average ^{230}Th fluxes during the Holocene and LGM, details are given in the auxiliary material. In the $\Psi_{Holocene}$ column, "none" indicates that no Holocene sediment was found in the core. For a rigorous discussion of the uncertainties inherent in the calculation of focusing factors, see *Kienast et al.* [2007].

[b]Unpublished data.

[c]Values from *McGee et al.* [2007] are averages since the LGM as described by these authors.

that ^{230}Th is preferentially removed in areas of high particle flux, such as at the equatorial Pacific [*Thomas et al.*, 2000; *Lyle et al.*, 2005]. Removing ^{230}Th from the water column reduces the concentrations of dissolved ^{230}Th in areas of high particle flux. In turn this encourages the addition of ^{230}Th by lateral mixing from areas of lower particle flux toward areas of high particle flux. We define this as the "particle flux effect"; this is sometimes referred to as "boundary scavenging" but we prefer the term "particle flux effect" to distinguish this process from additional processes which happen at ocean margins (see section 2.2 for discussion). It has been suggested that the particle flux effect leads to the high values in ^{230}Th flux observed at the equatorial Pacific and that such observations are not a result of sediment focusing [*Thomas et al.*, 2000; *Lyle et al.*,

2005]. Previous modeling work has concluded that the particle flux effect may account for increases in ^{230}Th flux to the sediment of up to 30% compared to the ^{230}Th input from the overlying water column (equivalent to a focusing factor of 1.3) [*Henderson et al.*, 1999]. However, those results would not allow for focusing factors of between 1.6 and 4.9, as observed in the equatorial Pacific (see below and Table 1), via the particle flux mechanism.

[5] We consider results from an equilibrium scavenging model for ^{230}Th within the Bern3D model, an ocean circulation model based on simplified ocean dynamics on which we impose fluxes of biogenic particles from the surface (Figure 1). Like the model presented by *Henderson et al.* [1999] our model explicitly takes into account the lateral transport of ^{230}Th in the water column. The model
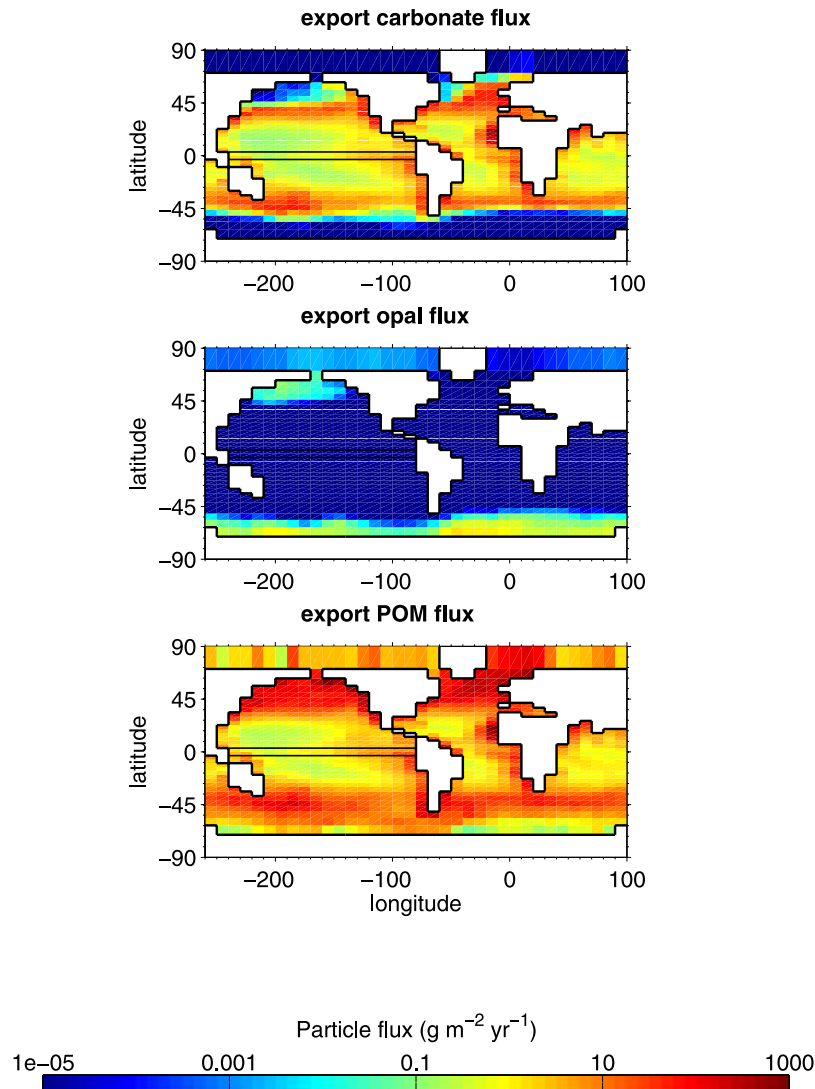
Figure 1. Particle fluxes used for the control run (annual mean values). The changes to the particle fluxes in the experiments described in the text are applied between the black lines at the equator. Dissolution of $CaCO_3$ with respect to depth is described by an exponential penetration profile; dissolution of POC with respect to depth is described by a power law; and dissolution of biogenic opal is described by a temperature-dependent (rather than depth-dependent) dissolution scheme, which gives near vertical profiles at high latitude. Particles are subject to a uniform settling rate across all particle types; no distinction is made for particles of different size classes.

reproduces observed water column [230]Th (Figure 2), giving us confidence in the ability of the model to represent the lateral transport of [230]Th in both the dissolved and particulate phase. Furthermore, the model has already been successfully used to simulate the particle flux effect for [231]Pa/[230]Th [*Siddall et al.*, 2005, 2007]. In other words, the model represents the particle flux effect to a reasonable degree. In sensitivity tests we consider a broad range of scavenging parameters with the effect of varying the water column concentrations of [230]Th and variations of the isopycnal diffusion parameter to examine the sensitivity of the particle flux effect on diffusive lateral transport. We vary the isopycnal diffusion for all tracers, including temperature and salinity. Because temperature and salinity (and therefore

density) vary in this way these experiments have slightly different ocean circulation compared to the control simulation and give some insight into the sensitivity of our approach to the precise ocean circulation that we apply. Within the ranges of our sensitivity tests we investigate whether or not the particle flux effect may explain the observed focusing factors in the equatorial Pacific. We follow a similar approach to the work of *Henderson et al.* [1999] but with the specific goal of considering the effects in the equatorial Pacific and comparing the model output to estimates of "focusing factors" based on observations. We expand on the work of *Henderson et al.* [1999] by considering the consequences of much increased particle fluxes at the equatorial Pacific on the particle flux effect. We com-
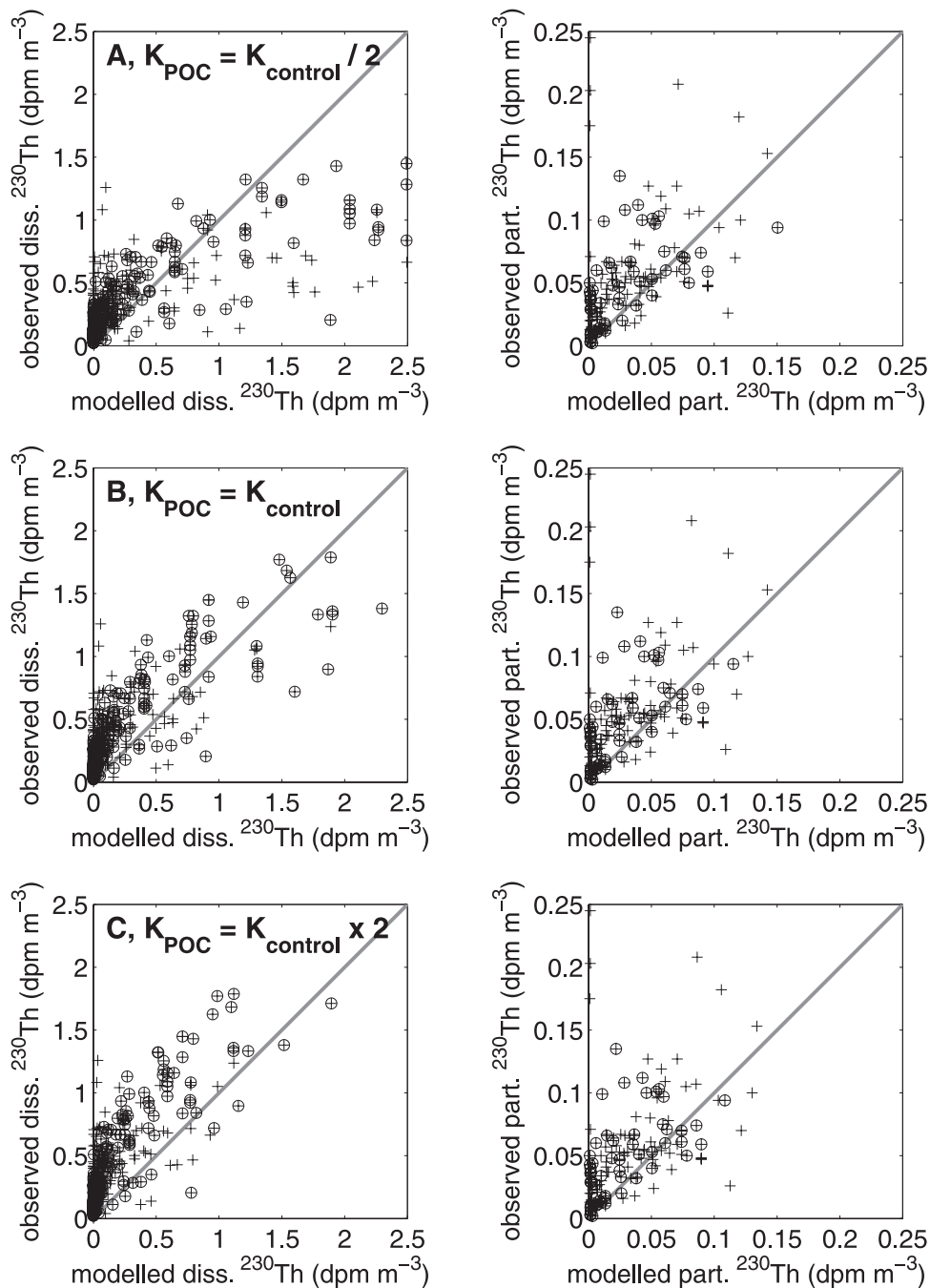
Figure 2. Sensitivity tests as described in the text for (a) $K_{POC} = K_{control}/2$; (b) $K_{POC} = K_{control} = 5 \times K_{ref}$ (the control run) and; (c) $K_{POC} = K_{control} \times 2$. (left) Comparison of modeled versus observed dissolved ^{230}Th values. (right) Comparison of modeled versus observed particulate ^{230}Th values. Sources for the data shown in the plot are cited by *Siddall et al.* [2005]. The circled crosses represent the Pacific data set, and the uncircled crosses represent the global data set.

pare the model output to observed focusing factors both for the present day and for the Last Glacial Maximum (LGM).

2. Method

[6] To summarize, assuming no particle flux effect the ratio of ^{230}Th accumulation in the sediment to its rate of production in the overlying water column is 1. However, the rate of ^{230}Th accumulation in the sediment can exceed its production in the water column either by lateral redistribution of sediments (sediment focusing), or by net lateral transport of ^{230}Th in the water column, from regions of low particle flux to regions of high particle flux via mixing processes (the particle flux effect) or via advection. We use a modeling approach to put upper limits on the particle flux effect. By comparing the observed focusing factors with the

modeled particle flux effect we place constraints on the proportional contribution to ^{230}Th accumulation by sediment focusing and the particle flux effect. In this section we describe the calculation of observed focusing factors, the Bern3D model, the representation of ^{230}Th in the model and the sensitivity tests, which we use to constrain the particle flux effect.

2.1. Calculation and Uncertainty of Observed Focusing Factors

[7] Focusing factors are calculated by dividing the total excess ^{230}Th inventory ([^{230}Th$_{xs}$], measured in disintegrations per minute (dpm) g^{-1}) in a given interval of a sediment core by the amount of ^{230}Th produced in the water column over the corresponding period of time (P_{Th}, measured in dpm cm^{-2} s^{-1}). The term "excess" is used to indicate that the values have been corrected for ^{230}Th originating from U decay within the detrital particles of the sediments, postdepositional decay of ^{230}Th and ^{230}Th supported by authigenic U in the sediments. Thus the excess ^{230}Th should uniquely reflect the ^{230}Th adsorbed from the water column. Average values for the dry bulk densities (ρ_b, measured in g cm^{-3}) are used to calculate the mean Ψ over dated intervals (t_1-t_2, measured in s). The durations of these intervals are defined by ^{14}C derived ages unless otherwise noted. In the case of data from *McGee et al.* [2007] the intervals are defined by age models derived from planktic δ^{18}O record on the same cores. The focusing factor, Ψ, is calculated as

$$\Psi = \frac{\int_{r_2}^{r_1} \left[{}^{230}\mathrm{Th}_{xs}\right]\rho_b dr}{P_{Th}(t_1 - t_2)}, \qquad (1)$$

where r is the depth in the core measured in cm. Table 1 shows the published and unpublished estimates of focusing factors (Ψ) used in this paper. Table S1 in auxiliary material summarizes the information used to make this calculation.[1]

[8] We make use of these observed focusing factors in two ways: (1) to make a general global comparison between the modeled particle flux effect and observed focusing factors and (2) to make a detailed (spatially resolved) comparison between the modeled particle flux effect and observed focusing factors in the equatorial Pacific. We will define the particle flux effect in our model as the ^{230}Th flux to the sediment normalized to ^{230}Th production in the water column at a given site.

[9] The calculation of accurate focusing factors remains a challenging task and there has been extensive discussion on the uncertainty in deriving focusing factors in the literature [see, e.g., *Marcantonio et al.*, 2001; *McGee et al.*, 2007; *Francois et al.*, 2007; *Kienast et al.*, 2007]. Uncertainties may originate from uncertainty in the estimates for dry bulk density or from the age models derived from the oxygen isotope stratigraphy in the deep Pacific [*Marcantonio et al.*, 2001; *Skinner and Shackleton*, 2005; *Kienast et al.*, 2007]. *Broecker et al.* [2006] have pointed out interspecies differ-

ences in radiocarbon age estimates of as much as 1000 years in the deep Pacific leading to uncertainty in radiocarbon derived age models. One might therefore ask whether the high focusing factors observed at the equatorial Pacific may be best explained by uncertainties in the variables in equation (1). In the following paragraph we discuss this question.

[10] *Kienast et al.* [2007] largely focused on the uncertainty of the calculation of focusing factors in the equatorial Pacific for a number of individual cores. For example, these authors revised the focusing factor for core Y69–71 to between 4.4 and 2.6 from the previously published value of 8.2 [*Loubere et al.*, 2004]. This example is the largest change to the revised focusing factors given by *Kienast et al.* [2007]. We note that, even with such a large reduction, this focusing factor is still impossible to explain in terms of the previous, model-based estimate of the particle flux effect, which is equivalent to a maximum focusing factor of 1.3 [*Henderson et al.*, 1999]. The *Kienast et al.* [2007] work is illustrative of the detailed knowledge of each individual core record of ^{230}Th, which is needed to understand the uncertainty in each individual estimate of the focusing factor. Here we focus on the broader scale of the whole equatorial Pacific region and not the detailed uncertainty in each estimate for the focusing factor.

[11] Although the uncertainties in the observed focusing factors given in Table 1 are likely to be large [e.g., *Marcantonio et al.*, 2001; *McGee et al.*, 2007; *Francois et al.*, 2007; *Kienast et al.*, 2007], we point out that it does not appear likely that Ψ varies systematically with the particle flux, unlike the particle flux effect. A more sophisticated treatment of the uncertainty involved in the calculation of focusing factors is beyond the scope of this paper but we note that even the most rigorous and carefully revised estimates of focusing factors at the equatorial Pacific to date (i.e., the values given by *Kienast et al.* [2007]) give values between 1.6 and 4.9 and cannot be explained by published estimates of the particle flux effect (1.3 [*Henderson et al.*, 1999]). The additional observational estimates of the particle flux effect given here all fall below the largest estimate from *Kienast et al.* [2007] of 4.9 (our observational range for the whole globe is 0.7 to 4.9) and so we feel confident that the additional values we provide are in a reasonable range. Given that focusing factors in the carefully revised data set of *Kienast et al.* [2007] are too large to be explained by the particle flux effect we reject the notion that the uncertainty in the calculation of focusing factors leads to the systematically high estimated focusing factors observed in the equatorial Pacific.

2.2. Bern3D Model

[12] The Bern3D model used in this work has been discussed in detail by *Müller et al.* [2006] and *Siddall et al.* [2005]. It transports tracers such as ^{230}Th via processes of advection, diffusion and convection [*Müller et al.*, 2006]. The Bern3D model is a computationally efficient ocean model of intermediate complexity based on the frictional geostrophic equations [*Edwards and Marsh*, 2005]. The model resolution is 36 by 36 grid squares of equal area across the globe in the horizontal plane with 32 depth levels.

The Bern3D model simulates the large-scale circulation on seasonal and longer timescales reasonably well (for detailed discussion see *Müller et al.* [2006]). The simulations shown in this paper all represent steady state solutions; we vary the particle fluxes with respect to modern estimates as well as the scavenging parameters as discussed below.

[13] The general merits and limitations of an intermediate complexity approach have been discussed at length elsewhere [e.g., *Marchal et al.*, 2000; *Siddall et al.*, 2006] and so here we limit our discussion to this specific study. The relatively high vertical resolution (32 depth levels) of our model has been specifically chosen to optimize the representation of equatorial upwelling [*Müller et al.*, 2006] and is therefore well suited to this study. Smaller-scale features of the oceanic transport processes in the equatorial Pacific reach scales of tens to hundreds of kilometers and are not resolved by the Bern3D model. In fact such features are only truly represented in the most complete, eddy resolving, primitive equation models. The integration time of such models would be prohibitive for the study considered here for which a large number of sensitivity tests are necessary.

[14] In line with many other models, subgrid-scale features in the Bern3D model are represented by isopycnal diffusive transport and a Gent-McWilliams transport parameterization [*Griffies*, 1998]. In order to test the sensitivity of our results to this parameterization we double and halve the isopycnal diffusion in the model to allow for uncertainty in the model representation of horizontal eddy mixing in the equatorial Pacific. We vary the isopycnal diffusion for all tracers, including temperature and salinity. Because we vary temperature and salinity in this way these experiments have slightly different ocean circulation compared to the control simulation and give some insight into the sensitivity of our approach to the precise ocean circulation that we apply.

[15] It is worth noting that the residence time of ^{230}Th in the ocean is several decades [*Henderson et al.*, 1999; *Henderson and Anderson*, 2003]. The effects of short-lived, small-scale features in the ocean circulation on ^{230}Th are therefore likely to be integrated over time; ^{230}Th is likely to be well mixed compared to the time and space scales of ocean eddies. Also worth noting is that the most dynamic, smaller-scale features of the equatorial ocean circulation are limited to the upper, wind-mixed layers, where ^{230}Th concentrations are very low. More significant to the ^{230}Th distribution is perhaps the sluggish, larger-scale circulation in the deep ocean, where ^{230}Th concentrations are high. This deep circulation is relatively well represented in the model. We emphasize that our results compare well with similar studies that have used other models [*Henderson et al.*, 1999; *Marchal et al.*, 2000], demonstrating that our results are insensitive to the detailed circulation in the model used.

[16] Particle fields are prescribed using satellite-derived export productivity fields and appropriate dissolution profiles for three particle types: biogenic opal; CaCO$_3$ and; particulate organic carbon (POC). Because particle dissolution in the model is discussed in detail by *Siddall et al.* [2005], here we provide only a brief description: dissolution of CaCO$_3$ with respect to depth is described by an exponential penetration profile; remineralization of POC with respect to depth is described by a power law; and dissolu-

tion of biogenic opal is described by a temperature-dependent (rather than depth-dependent) dissolution scheme, which gives near vertical profiles at high latitude. Similar to previous work [*Henderson et al.*, 1999; *Marchal et al.*, 2000; *Siddall et al.*, 2005, 2007], particles are subject to a uniform settling rate of 1000 m a^{-1} across all particle types; no distinction in settling rate is made for particles of different size classes. Given that the residence time of ^{230}Th in the ocean is several decades we assume that it is not sensitive to seasonal fluctuations in the particle flux and apply an annual mean settling rate. This does not allow for rapid "marine snow" events but captures the mean particle flux to the sediment. Sensitivity tests regarding the settling velocity are discussed below. *Siddall et al.* [2005] found that scavenging of ^{231}Pa and ^{230}Th by dust was not significant in controlling the broad pattern of ^{231}Pa and ^{230}Th distribution in the ocean. In addition, the dust flux at the equatorial Pacific is estimated to be 2 orders of magnitude lower than the flux of biogenic particles and so the dust flux is neglected for the purpose of the present study. Present-day particle fields are shown in Figure 1.

2.3. The ^{230}Th Partition Coefficients

[17] A reversible scavenging model is applied to ^{230}Th so that the process of adsorption onto falling particles and subsequent desorption at depth leads to an increase of ^{230}Th activity in the water column with depth [*Bacon and Anderson*, 1982; *Roy-Barman et al.*, 1996]. Within such a scheme adsorption/desorption take place because of the sinking of particles to depths with different ^{230}Th concentrations and because of particle dissolution. Nuclide adsorption/desorption processes linked to particle aggregation and disaggregation are not considered explicitly. An equilibrium-scavenging coefficient is used to describe the relationship between adsorbed and desorbed isotopes. This model assumes that ^{230}Th in the water column is at equilibrium with falling particles. Such equilibrium-scavenging coefficients have often been used to describe the relationship between adsorbed and desorbed ^{230}Th [*Henderson et al.*, 1999; *Chase et al.*, 2002; *Luo and Ku*, 1999, 2004a, 2004b; *Li*, 2005; *Siddall et al.*, 2005]. K is defined as the ratio between dissolved, A_d, and particle-associated, A_p, activity:

$$K_p = \frac{A_p}{A_d C_p}. \tag{2}$$

Here C_p (dimensionless) is the ratio between the particle mass per cubic meter of water and the water density. Because A_p and A_d are both in units of dpm m^{-3}, K is dimensionless. The subscript p represents the particle type (POC, CaCO$_3$ or opal). K values for separate particle types have proved difficult to observe directly [*Honeyman et al.*, 1988] and it is uncertain how readily laboratory assessment of their values [*Geibert and Usbeck*, 2004] can be extrapolated to the field. Modeling work is consistent with the observational assertion [*Chase et al.*, 2002] that the global ^{230}Th distribution in the ocean is largely controlled by the global distribution of the biogenic opal compared to CaCO$_3$ flux to the ocean sediments [*Marchal et al.*, 2000; *Siddall et al.*, 2005], the magnitude of the particle flux

Table 2. List of Equilibrium-Scavenging Coefficients (*K*) Used in This Study as Adapted From *Chase et al.* [2002] and Following *Siddall et al.* [2005, 2006]

Variable	Symbol	Control
Equilibrium-scavenging coefficient	K_{ref}	10^7
^{230}Th scavenging by CaCO$_3$	K_{car}^{Th}	K_{ref}
^{230}Th scavenging by opal	K_{opal}^{Th}	$K_{ref}/20$
^{230}Th scavenging by dust	K_{dust}^{Th}	0
Control value for ^{230}Th scavenging by POC	$K_{control}$	$5 \times K_{ref}$
Sensitivity tests for ^{230}Th scavenging by POC	K_{POC}^{Th}	$K_{control}/2$, $K_{control} \times 2$

[*Bacon et al.*, 1976; *Anderson et al.*, 1983, 1990] and deep ocean advection [*Marchal et al.*, 2000; *Siddall et al.*, 2005].

[18] Values for equilibrium partition coefficients used in this study are given relative to a reference value which is approximately equivalent to the partition coefficient of ^{230}Th with respect to CaCO$_3$ ($K_{ref} = 1 \times 10^7$) [*Chase et al.*, 2002]. Values for equilibrium partition coefficients used in this paper are summarized in Table 2.

[19] Boundary scavenging is the range of processes by which particle-reactive elements are preferentially removed to the sediment at ocean margins, including both high particle flux and particle type effects [*Bacon et al.*, 1976; *Anderson et al.*, 1983, 1990]. High lithogenic flux from rivers and coastal erosion provide a primary source of additional particulate flux for scavenging. The supply of nutrients from rivers increases primary productivity, in turn also increasing the particulate flux available for scavenging close to the coasts. High-productivity upwelling zones near the coast are approximated in the model but there is no representation of the input of lithogenic material at the coast. Boundary scavenging is effectively represented in the model only by the effect of higher productivity related to upwelling areas in grid boxes close to the coast.

[20] The potential effect of nepheloid layers on ^{230}Th is not considered. Redissolution of ^{230}Th from the surface sediment is not considered and is not thought to be significant [*Francois et al.*, 2007]; sensitivity tests regarding this effect are discussed below. There has been some suggestion that particle size classes may scavenge differentially and that particles in smaller size classes cannot sink without undergoing aggregation. The significance of this point is that particles in smaller size classes may be transported around the ocean along with the ^{230}Th associated with them [*Lyle et al.*, 2005]. Both particle-associated and dissolved ^{230}Th are transported in the model and so the model takes this process into account. The model does not explicitly account for any removal to the sediment of ^{230}Th attached to the smallest particle size. Our model simulates the modern sedimentary ^{231}Pa/^{230}Th distribution reasonably well [*Siddall et al.*, 2005, 2007]. The significance of this point is that the ocean ^{231}Pa/^{230}Th distribution is highly sensitive to the particle flux effect and so we feel justified in applying it here.

2.4. Sensitivity Tests

[21] Our goal is to quantify the particle flux effect at the equatorial Pacific within reasonable bounds. In order to design sensitivity tests appropriate to this goal we need to vary the water column concentrations of ^{230}Th. We achieve this by varying the total scavenging of ^{230}Th. Because the particle flux effect is dependent only on the water column concentration of ^{230}Th our approach is independent of the particle type for which we vary the scavenging, i.e., the results presented here are independent of which particle type we use for the sensitivity test. The sensitivity tests carried out for *Siddall et al.* [2005] demonstrate that this is indeed the case and our result is independent of the particle-type effect. *Chase et al.* [2002] used a global data set and an end-member model to constrain the scavenging coefficients for opal and CaCO$_3$ for ^{230}Th but could not resolve the scavenging coefficient for POC, which remains poorly constrained. We therefore choose to vary the ^{230}Th scavenging coefficient of POC as an effective and pragmatic means to vary the total scavenging and ^{230}Th residence time in the model while bringing the modeled concentrations of ^{230}Th in the water column into line with observations. We emphasize once more that varying any of the scavenging parameters achieves the same result; this effect appears robust at the equatorial Pacific where the spatial variation in each of the biogenic particle types follows a similar pattern (Figure 1). A value for the ^{230}Th scavenging coefficient of POC of $5 \times K_{ref}$ closely reproduces the dissolved ^{230}Th concentrations in the water column (Figures 2 and 3) with an r squared value of 0.8 (note that this should be regarded a the "operational value" for use in this paper and not a precise estimate). We define this value as $K_{control}$ (i.e., $K_{control} = 5 \times K_{ref} = 5 \times 10^7$). Halving this control value leads to an excess of dissolved ^{230}Th in the water column compared to observations (Figure 2a). Correspondingly, doubling the control ^{230}Th scavenging coefficient of POC leads to a deficit of dissolved ^{230}Th in the water column compared to observations (Figure 2c). These sensitivity tests lead to a range of between 13 and 33 years for the residence time (residence times calculated by dividing the total ^{230}Th inventory by the total rate of ^{230}Th production in the ocean) of ^{230}Th in the ocean, in good agreement with estimates from other models and from observations (Table 3).

[22] Consistent with many other models, subgrid-scale features in the Bern3D model are represented by isopycnal transport and a Gent-McWilliams transport parameterization [*Griffies*, 1998]. In the control simulation the isopycnal diffusion (I) is set to 1000 m^2 s^{-1}. In order to test the sensitivity of our results to this parameterization we double (I = 2000 m^2 s^{-1}) and halve (I = 500 m^2 s^{-1}) the isopycnal diffusion in the model to allow for uncertainty in the model representation of horizontal eddy mixing in the equatorial Pacific.

[23] *Lyle et al.* [2005] argued that the leakage of ^{230}Th from slowly accumulating sediments would promote the lateral transport of ^{230}Th within the water column. *Francois et al.* [2007] demonstrated that an input of ^{230}Th as a result of leakage from the sediments would generate a spike in ^{230}Th at the bottom of the water column, in disagreement
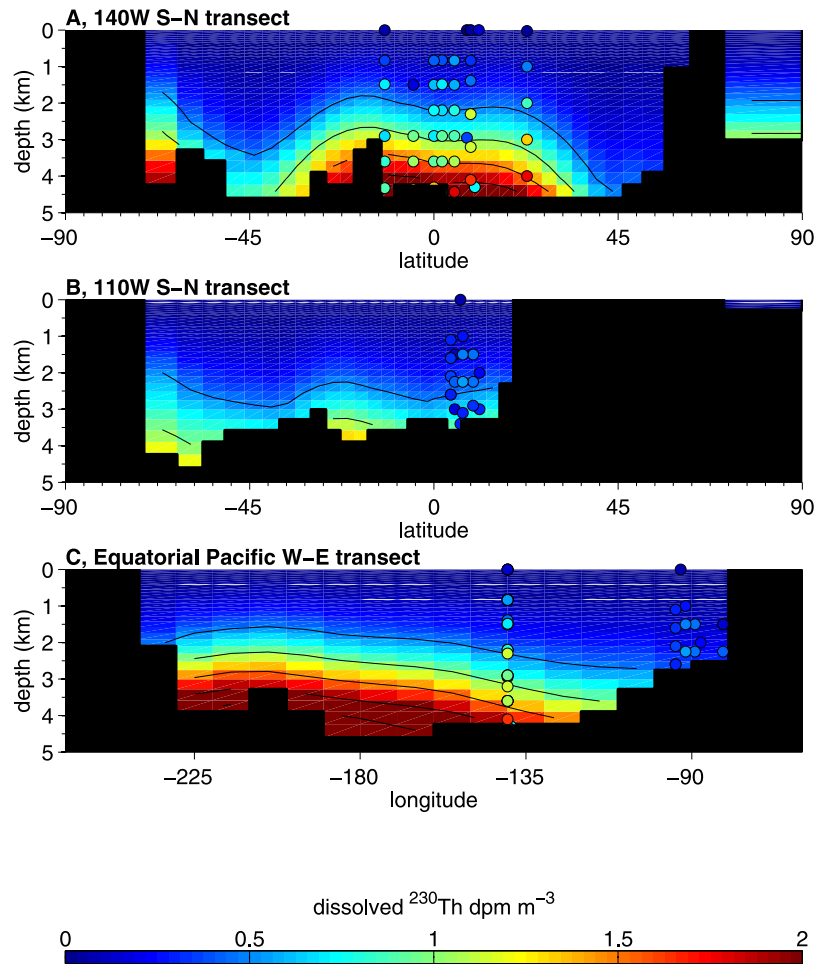
Figure 3. Distribution of dissolved ^{230}Th at the equatorial Pacific in the control run compared to observed values (circles) in three transects: (a) south-north transect at 140°W, (b) south-north transect at 110°W, and (c) west-east transect along the equator. Sources for the data shown in the plot are *Moore* [1981], *Bacon and Anderson* [1982], *Nozaki and Nakanishi* [1985], *Roy-Barman et al.* [1996] and R. F. Anderson and M. Q. Fleisher (unpublished data, 1993, http://usjgofs.whoi.edu/jg/dir/jgofs/eqpac/tt013/). Black contours are at increments of 0.5 disintegrations per minute (dpm) m^{-3} from 0.5 to 2 dpm m^{-3}.

with observations and effectively ruling out the suggestion. We have carried out simulations with an additional source of ^{230}Th due to leakage from the sediments by redissolving 50% of the ^{230}Th input to the sediment each time step. These simulations generated very little additional ^{230}Th in the water column because the ^{230}Th input was quickly removed via increased reversible scavenging, rather than diffusing upward into the water column. Rapid scavenging

Table 3. A Compilation of Published Residence Time Estimates for ^{230}Th From Observations and Models

Reference	Observations/ Model	^{230}Th Residence Time, years
This paper: control run, $K_{POC}^{Th} = K_{control} = K_{ref} \times 5$	model	19
This paper: $K_{POC}^{Th} = K_{control}/2$	model	33
This paper: $K_{POC}^{Th} = K_{control} \times 2$	model	13
Henderson and Anderson [2003]	observations	20
Yu et al. [1996]	observations	30
Anderson et al. [1983]	observations	10–50

to the sediment prevented significant lateral transport in these simulations. As noted above, the simulation in which we halve the ^{230}Th scavenging coefficient of POC leads to an excess of dissolved ^{230}Th in the water column compared to observations (Figure 2a). This simulation may be considered as a (unrealistic) limiting case for which additional sources of ^{230}Th diffuse upward rapidly following leakage from the sediments.

[24] *Siddall et al.* [2005] used the same numerical model as that applied here as well as an analysis of the scavenging equations to show that one should not expect there to be any effect on water column ^{230}Th concentrations from varying the particle settling velocity. Instead the water column ^{230}Th concentration varies with the scavenging coefficient, the particle flux and depth. For the sake of rigor we have carried out a series of sensitivity tests to check if changes in the particle settling velocity affect our results in the equatorial Pacific and find that indeed there is no effect on the ^{230}Th concentration (we varied the settling velocity between 500 and 1500 m a^{-1}). Because the particle flux effect depends

on the water column [230]Th concentration there is no change to the particle flux effect as a result of changing the particle settling velocity. This is as one would anticipate from previously published results [i.e., *Siddall et al.*, 2005] and so the sensitivity tests are not shown here.

3. Results

3.1. Sediment Focusing Versus the Particle Flux Effect

[25] Figure 4 (left) shows the modeled particle flux effect (i.e., the [230]Th flux to the sediment normalized to the water column production) for the three cases of varying K_{POC} (i.e., $K_{POC} = K_{control}$, $K_{POC} = K_{control}/2$ and $K_{POC} = K_{control} \times 2$) in comparison with the observed focusing factors (Table 1). Given that this wide range of parameter space effectively

bounds the water column [230]Th inventory it is reasonable to assume that the model captures the particle flux effect. It is interesting to note that even for large changes in the dissolved [230]Th in the water column (Figures 2 and 3), there are only minor changes in the particle flux effect (Figure 4 right). The simulated particle flux effect maxima range from 1.36 to 1.57 and the minima range from 0.49 to 0.82 in the three experiments (Figure 4). Although the model simulates observed water column [230]Th concentrations, none of the sensitivity tests varying K_{POC} are capable of simulating the observed focusing factors. Because the observed focusing factors are too large to be explained by the model we conclude that it is unlikely that the particle flux effect can fully account for the high focusing factors observed at the equatorial Pacific.
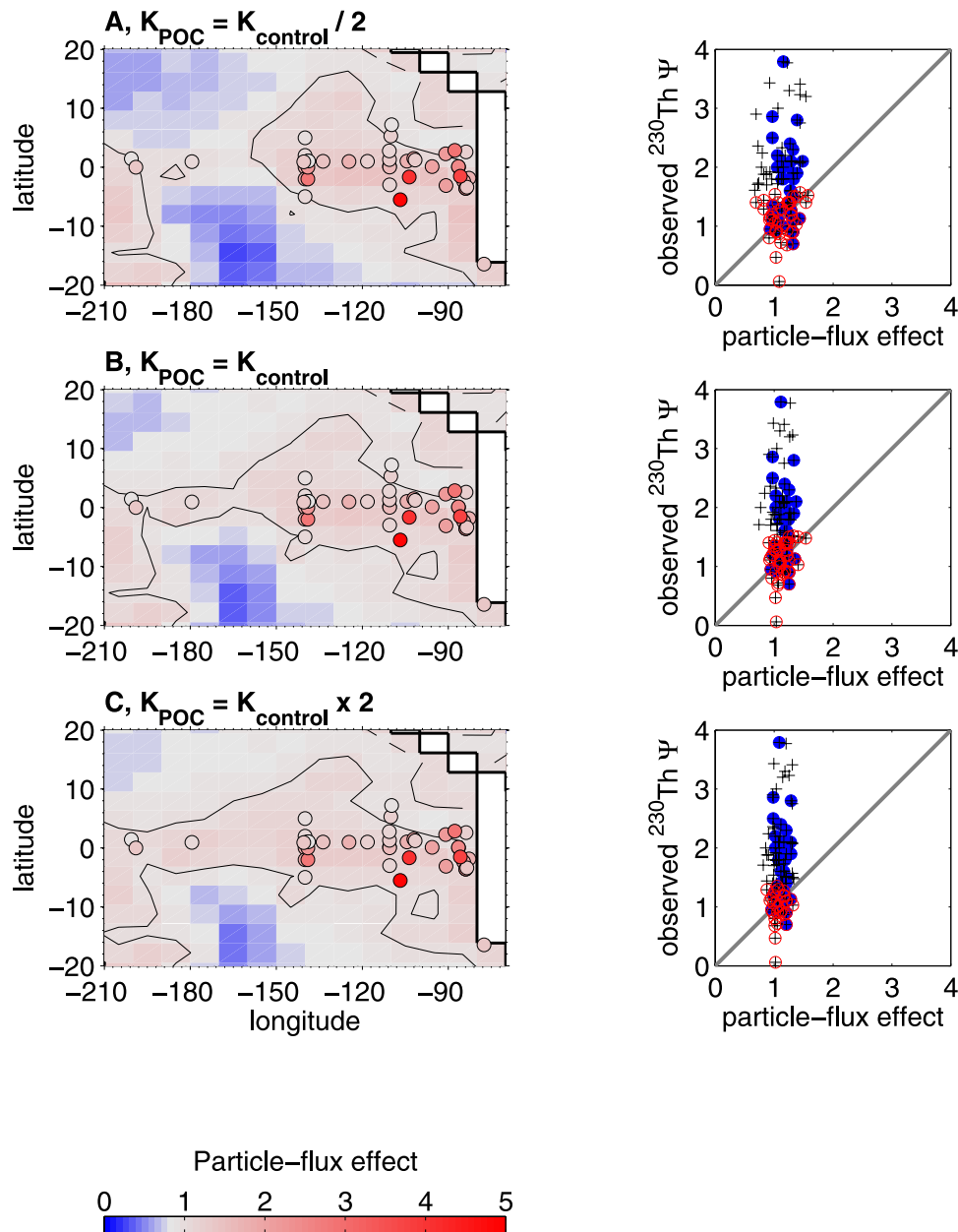

Figure 4

[26] Figure 4 illustrates that the large range covered by the observed focusing factors is not captured by the model. The large range in focusing factors observed at the equatorial Pacific is consistent with processes that involve regional- to local-scale sediment focusing (which are not represented in the model), but the observed variability between sites is not consistent with the systematic pattern of reduced variability that would be expected if the particle flux effect were the dominant factor responsible. This result supports the conclusion of *Francois et al.* [2007] and it seems likely that indeed sediment focusing is at least in part responsible for the high focusing factors at the equatorial Pacific.

[27] The effect of varying the isopycnal diffusion by a factor of 2 (i.e., doubling and halving I) is shown in Figure 5. The impact of this change in I is similar to the sensitivity tests halving and doubling the scavenging of ^{230}Th by POC. The reason for this is that halving K_{POC} increases the residence time of ^{230}Th in the water column and thereby the exposure of ^{230}Th to the effects of horizontal mixing and doubling the horizontal mixing in the water column has a similar effect. The inverse is also true: increasing K_{POC} decreases the residence time of ^{230}Th in the water column which reduces horizontal mixing in a similar way to reducing I. This effect can be seen in the model results shown in Figures 4 and 5 (right); the maximum particle flux effect is found by halving K_{POC} and doubling I and this minimum particle flux effect is given by doubling K_{POC} and halving I.

[28] These sensitivity tests illustrate an important point in our model: it is the ratio between the horizontal mixing and the residence time that are the key factors in determining the particle flux effect. There is an asymptotic maximum limit on the particle flux effect with respect to the residence time (i.e., here achieved by reducing K_{POC}) and horizontal mixing (i.e., here achieved by increasing I). Doubling I or halving K_{POC} pushes the particle flux effect to that limit. Halving I or doubling K_{POC} leads to a reduction in the particle flux effect toward the value of 1 in the equatorial region (i.e., no particle flux effect). It is these limits which explain why ^{230}Th is a robust proxy for constraining particle rain rates.

3.2. Varying Particle Fluxes Over Time
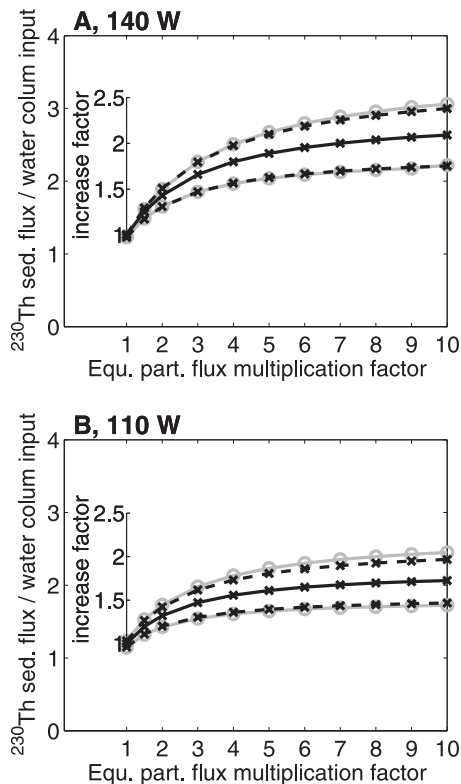
[29] Because the ^{230}Th normalized particle fluxes are commonly used to calculate down-core variations in rain rate, it is interesting to consider how the particle flux effect might change with increasing particle fluxes along the equatorial Pacific. We consider the extreme case of increasing all particle flux types only in the grid boxes that immediately juxtapose the equator in the Pacific. In this way the particle flux effect is maximized because there is a very sharp gradient between the zone of high particle flux and the zone outside of it (the particle flux effect is thought to be largely controlled by the gradient in particle flux). Simulations were run for a large range of particle fluxes, increasing the equatorial particle flux up to a factor of 10. Even in such an extremely unrealistic case the maximum possible impact is to enhance the particle flux effect by a factor of 2 at 140°W, and a factor of 1.6 at 110°S, relative to the control run (Figure 6). A maximum increase of a factor of 2.5 is observed at 140°W if the isopycnal diffusion is set to the large value of 2000 m^2 s^{-1}. This would indicate that there is not likely to be a systematic bias in excess of a few tens of percent in down-core changes in particle flux derived by ^{230}Th normalization.

[30] Why does the particle flux effect change little with large increases in the particle fluxes? As discussed earlier (section 3.1), the particle flux effect is limited by the extent of horizontal mixing into the regions where ^{230}Th is removed (note that advective effects on ^{230}Th are not sensitive to particle flux). The limit on this effect is due to the relatively short residence time of ^{230}Th in the water column, which limits the extent to which it can be laterally transported before deposition. Increased particle fluxes further reduce the residence time of ^{230}Th, reducing the time available for the lateral transport of ^{230}Th in the water column and thereby limiting the particle flux effect. Figures 7b and 7c show large reductions in the water column dissolved ^{230}Th concentrations due to increasing the equatorial particle fluxes by a factor of 2 and 5, respectively. Figures 8b and 8c show that the same large increases in the equatorial particle fluxes only have a minor impact on the particle flux effect, illustrating that these large

Figure 4. Modeled particle flux effect (i.e., ^{230}Th inventories in the sediment normalized to ^{230}Th production in the water column above) is compared with observed focusing factors (Table 1) (left) at sites throughout the equatorial Pacific using model scavenging intensities set at (b) the control at $K_{POC} = K_{control} = 5 \times K_{ref}$, (a) below the control at $K_{POC} = K_{control}/2$ and (c) above the control at $K_{POC} = K_{control} \times 2$. Observed focusing factors (colored circles) include information about both ^{230}Th transport in the water column and transport in the surface sediment (sediment focusing). The thin black contour follows the modeled particle flux effect isoline with a value of 1. Values greater than one in the model indicate a lateral input of ^{230}Th in the water column, whereas values less than one indicate the lateral removal of ^{230}Th in the water column. (right) Comparison of the modeled particle flux effect versus observed ^{230}Th focusing factors for the Holocene (Table 1), using model output for the grid cell in which each observation falls. The blue circles represent the equatorial Pacific data set shown on the left, and the black crosses represent the remainder of the global data set. The points circled in red represent the range of values that could be explained by the particle flux effect (the data which fall within the range of the maximum and minimum of the model results). Points falling in this range could be explained either by sediment focusing or by the particle flux effect. Sources for the data shown in the plot are cited in Table 1. The model only includes ^{230}Th transport in the water column. The poor comparison between the model and many of the observed focusing factors suggests that ^{230}Th transport in the surface sediment (sediment focusing) makes a dominant contribution to the observed ^{230}Th focusing factors at many sites, both in the equatorial Pacific and elsewhere.
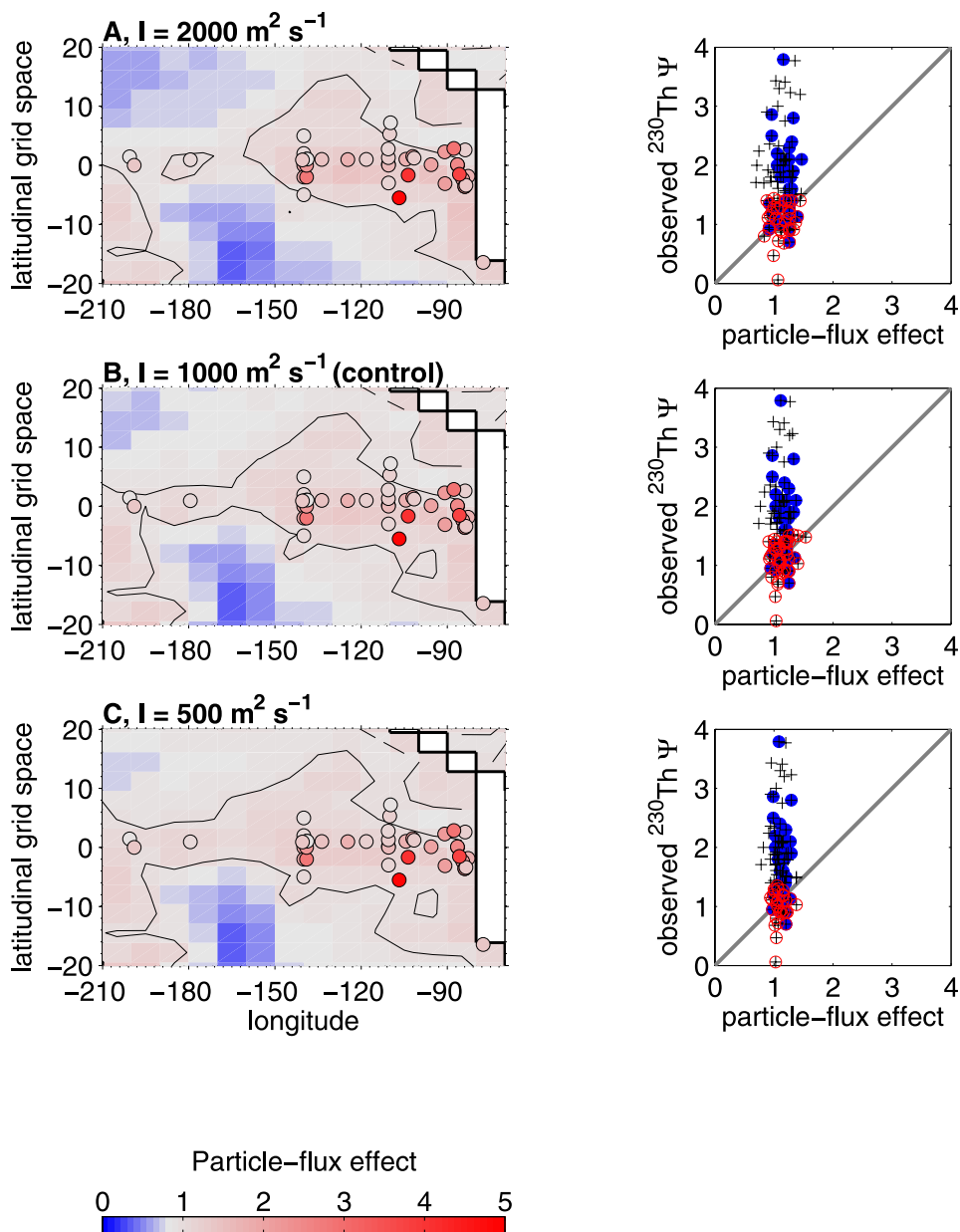
Figure 5. Modeled particle flux effect (i.e., ^{230}Th inventories in the sediment normalized to ^{230}Th production in the water column above) is compared with observed focusing factors (Table 1) at sites (left) throughout the equatorial Pacific using values for isopycnal diffusion set at (b) the control at I = 1000 m^2 s^{-1}, (a) above the control at I = 2000 m^2 s^{-1} and (c) below the control at I = 500 m^2 s^{-1} (see text). Observed focusing factors include information about both ^{230}Th transport in the water column and transport in the surface sediment (sediment focusing). The thin black contour follows the modeled particle flux effect isoline with a value of 1. Values greater than one in the model indicate a lateral input of ^{230}Th in the water column, whereas values less than one indicate the lateral removal of ^{230}Th in the water column. (right) Comparison of the modeled particle-flux effect versus observed ^{230}Th focusing factors for the Holocene. The blue circles represent the Pacific data set, and the black crosses represent the global data set. The points circled in red represent the range of values which could be explained by the particle flux effect (the data which fall within the range of the maximum and minimum of the model results); we underline that points falling in this range could be explained by either sediment focusing or the particle flux effect. Sources for the data shown in the plot are cited in Table 1. The model only includes ^{230}Th transport in the water column. The poor comparison between the model and many of the observed focusing factors suggests that ^{230}Th transport in the surface sediment (sediment focusing) makes a dominant contribution to the observed ^{230}Th focusing factors at many sites at the equatorial Pacific.

Figure 6. Modeled particle flux effect (i.e., the ^{230}Th flux to the sediment normalized to ^{230}Th production in the water column immediately above) at two sites on the equator in the Pacific. The equatorial particle fluxes are multiplied by the factor on the lower axes in each plot in the region shown in Figure 1. Two examples are shown: (a) 140°W and (b) 110°W. Sensitivity tests as described in the text are shown for the control run, $K_{POC} = K_{control} = 5 \times K_{ref}$ I = 1000 m^2 s^{-1} (solid black line); $K_{POC} = K_{control}/2$ (top dashed line); $K_{POC} = K_{control} \times 2$ (bottom dashed line); I = 2000 m^2 s^{-1} (top gray line) and; I = 500 m^2 s^{-1} (bottom gray line). The two scales on the left refer to the absolute change in ^{230}Th flux to the sediment normalized to ^{230}Th production (leftmost) and the change relative to the control or "increase factor" (rightmost).

changes in particle flux result in only small changes in ^{230}Th flux to the sediment even with isopycnal diffusion at double the control value (I = 2000 m^2 s^{-1}).

[31] Although not modeled here, we note that an effective means to increase the particle flux effect may be to further reduce the particle fluxes in regions of low particle flux, rather than increasing the particle fluxes in regions where they are already high. Following from this concept, Figure 6 reveals a relationship which asymptotes at higher values of the equatorial particle flux; doubling or tripling the particle flux corresponds to the largest changes in the ^{230}Th flux to the sediment but for further increases in the particle flux the relationship begins to plateau. As anticipated from the discussion in section 3.1 varying the horizontal mixing in the model has a similar effect to varying the total scavenging in the model.

[32] It is interesting to note that the site at 140°W has a greater sensitivity to changing particle flux compared to the 110°W site: the particle flux effect at 140°W shows an increase of a factor of ~2 while at 110°W it shows an increase of a factor of ~1.5 for a factor of 10 increase in the particle flux. This is because the dissolved ^{230}Th concentrations are higher in the central equatorial Pacific compared to the east (Figure 3). In turn this is due to increased particle fluxes which remove more ^{230}Th from the water column in the eastern part of the basin compared to the west (Figure 1). We suggest that the more westerly site may be more sensitive to changing particle fluxes in the past. Figures 8b
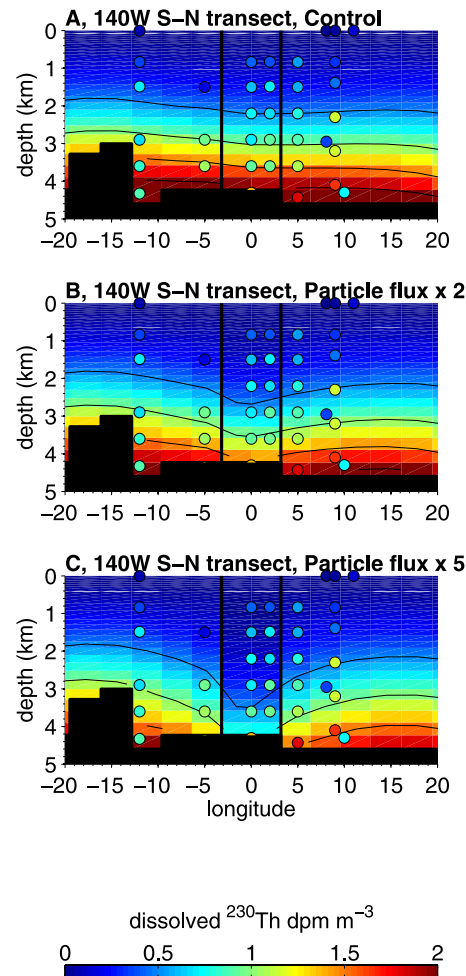
Figure 7. Distribution of dissolved ^{230}Th at the equatorial Pacific in the model compared to observed values (circles) for the three cases discussed in the text: (a) present-day particle flux, (b) twice the present-day particle flux around the equator and, (c) five times the present-day particle flux around the equator. Sources for the data shown in the plot are *Moore* [1981], *Roy-Barman et al.* [1996], and R. F. Anderson and M. Q. Fleisher (unpublished data, 1993, http://usjgofs.whoi.edu/jg/dir/jgofs/eqpac/tt013/). Particle fluxes are increased along the equator in the latitudinal band defined by black vertical lines in the plots. The isopycnal mixing is set at the control value of 1000 m^2 s^{-1}.
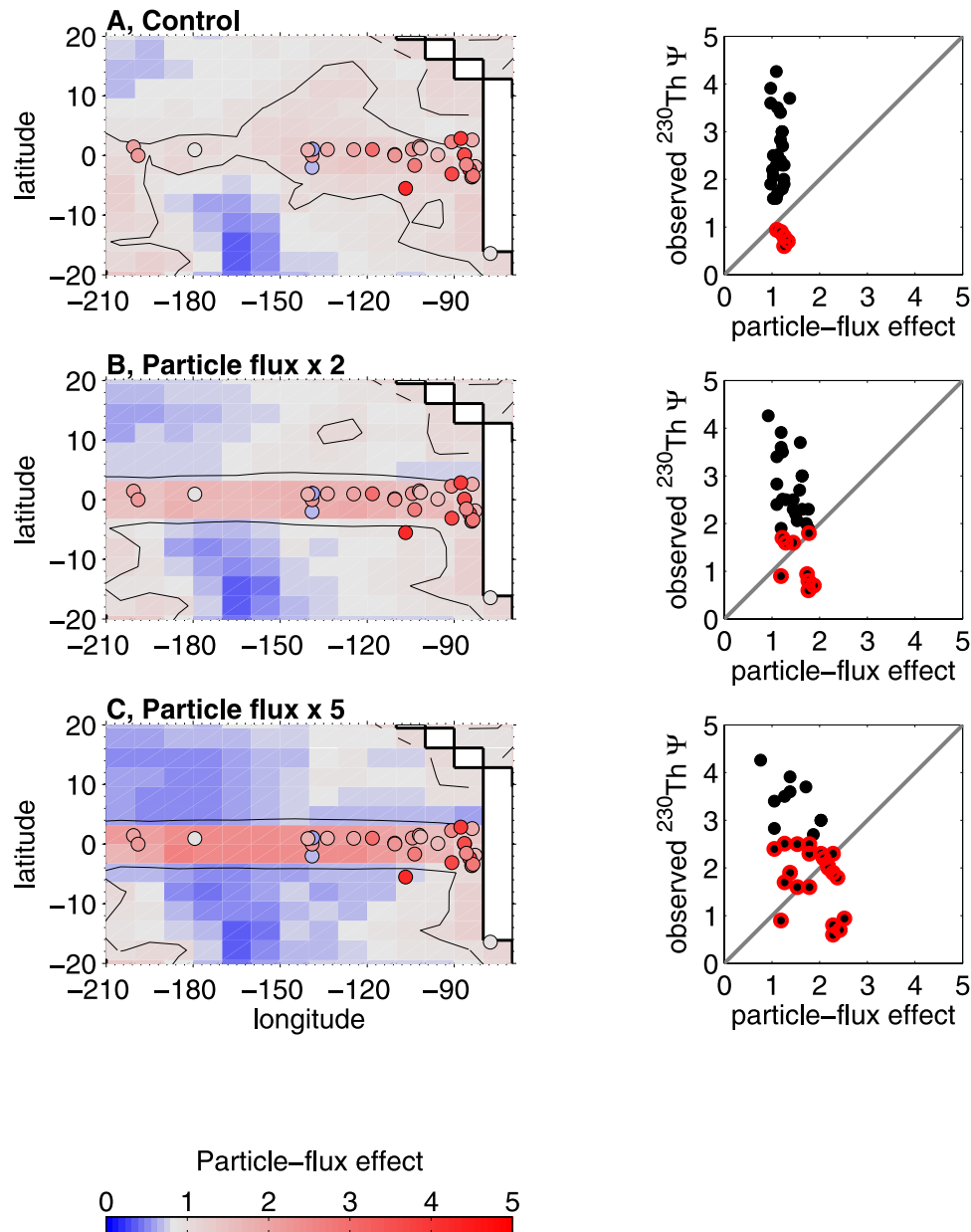
Figure 8. (left) Modeled particle flux effect (i.e., the [230]Th flux to the sediment normalized to [230]Th production in the water column immediately above) at the equatorial Pacific. Values greater than one indicate a lateral input of [230]Th in the water column, whereas values less than one indicate the lateral removal of [230]Th in the water column. Shown as colored circles with the same color scale are the focusing factors for the LGM calculated for samples taken from the equatorial Pacific (Table 1). Observed focusing factors include information about both [230]Th transport in the water column and transport in the surface sediment (sediment focusing). (right) Modeled particle flux effect versus observed [230]Th focusing factors for the LGM, where model results are plotted for the grid cell containing the corresponding core location. The points circled in red represent the range of values that could be explained by the particle flux effect (the data which fall within the range of the maximum and minimum of the model results). Points falling in this range could be explained either by sediment focusing or by the particle flux effect. Sources for the data shown in the plot are cited in Table 1 (observed focusing factors). Simulations as described in the text for (a) the control run (i.e., present-day particle flux), (b) twice the present-day particle flux around the equator, and (c) five times the present-day particle flux around the equator. Because the model only includes [230]Th transport in the water column, the poor comparison between the model and the observed LGM focusing factors indicates that [230]Th transport in the surface sediment (sediment focusing) makes a significant contribution to the observed [230]Th focusing factors at many sites at the equatorial Pacific.

and 8c show simulations for increasing the equatorial particle fluxes by a factor of 2 and 5, respectively. By comparing the modeled particle flux effect at the equatorial Pacific for the cases of increased particle flux in Figure 8, we confirm that the largest increases due to increasing particle fluxes at the equator are indeed found at the more westerly sites in the model.

[33] Also shown in Figure 8 are the observed focusing factors for the LGM (Table 1). It has been suggested that an increase in observed focusing factors in the eastern equatorial Pacific during the LGM compared to today results from increased particle flux during this period (which would enhance the particle flux effect) [Lyle et al., 2005]. However, the model results indicate that observed focusing factors often exceed the maximum ^{230}Th flux that can be attributed to the particle flux effect (Figure 8 right). For the case of a factor of 5 increase in the equatorial particle fluxes there is a slight improvement of the match between observed LGM focusing factors and the modeled particle flux effect. However, even for this extreme increase in the equatorial particle flux, the particle flux effect cannot fully explain the largest observed LGM focusing factors, of up to ~4.

4. Conclusions

[34] Our model lacks several features needed to fully represent ^{230}Th focusing in the deep ocean. As we better understand the dynamics of nepheloid layers, deep ocean currents and particle settling on slopes it will be interesting to make revised modeling approaches which take these into account. The inclusion of different particle size classes and the possible removal of ^{230}Th by particles in the smallest size class should be considered in the future. The removal of ^{230}Th from the water column by rapidly falling marine snow should also be considered, although our understanding of this process is limited at present. New approaches to integrating tracers in general circulation models such as the Transport Matrix Method [Khatiwala et al., 2005] are beginning to provide alternative, higher resolution means to study the distributions of tracers, overcoming some of the limitations of the intermediate complexity approach. Despite these limitations we are able to draw significant conclusions with regard to the particle flux effect and the use of ^{230}Th as a constant-flux proxy.

[35] Our model reproduces reasonably well the dissolved ^{230}Th concentrations in the equatorial Pacific and elsewhere in the ocean. We are therefore confident in the use of this model in understanding the particle flux effect, whereby ^{230}Th is removed preferentially in areas of high particle flux. In agreement with previous modeling work the particle flux effect typically increases the flux of ^{230}Th to the surface sediment by a factor of up to 1.3 compared to ^{230}Th production in the water column above a given site

[Henderson et al., 1999], in this case for the equatorial Pacific. Because our sensitivity tests have effectively parenthesized the observed water column concentrations of ^{230}Th we conclude that the particle flux effect is too small to explain a large proportion of the observed focusing factors in the equatorial Pacific, which range from 0.7 to 4.9 during the Holocene. Note that the rigorously revised subset of the data included here and published by Kienast et al. [2007] gives focusing factors ranging between 1.6 and 4.9, which are too large to be explained by the particle flux effect. In fact our sensitivity tests bound almost all of the observed concentrations of dissolved ^{230}Th (Figure 2 left) but there is almost no impact on the modeled ^{230}Th flux to the sediment at 140°W and 110°W (note the negligible difference between the solid line and the dashed lines for "particle flux multiplication factor" of 1.0 in Figure 6 and the similarity of the simulations shown in Figure 4).

[36] We also considered the effect of increasing the equatorial particle fluxes over a broad range (up to a factor of 10). Even for such large changes the particle flux effect changes the flux of ^{230}Th to the sediment by a factor of only 2 compared to ^{230}Th production in the water column above the site. We thus conclude that there is not likely to be a systematic bias in down-core ^{230}Th normalized particle fluxes driven by varying particle fluxes over time.

[37] Our simulations are inconsistent with the notion that increased particle fluxes at the LGM forced an increase in the particle flux effect over this period. The LGM focusing factors at the equatorial Pacific are not simulated even for very large increases in the particle flux.

[38] In the extreme case presented here the particle flux effect may reach a maximum of ~1.6 in the equatorial Pacific region. This offset coincides with the equatorial maximum in particle flux and may account for an offset in the absolute values in sediment accumulation calculated using ^{230}Th normalization. However, because the equatorial region is subject to persistently high particle fluxes, the sensitivity of the particle flux effect to increases in the particle flux is minimal, as we have shown. Any variation in the particle flux over time would not result in systematic biases in ^{230}Th normalization. We conclude that variation in the particle flux effect (due to variation in the magnitude of the particle flux) will not have a significant impact on the calculation of down-core sediment accumulation rates by ^{230}Th normalization.

References

Anderson, R. F., M. P. Bacon, and P. G. Brewer (1983), Removal of ^{230}Th and ^{231}Pa from the open ocean, *Earth Planet. Sci. Lett.*, *62*, 7–23, doi:10.1016/0012-821X(83)90067-5.

Anderson, R. F., Y. Lao, W. S. Broecker, S. E. Trumbore, H. J. Hofmann, and W. Wolfi (1990), Boundary scavenging in the Pacific Ocean: A comparison of ^{10}Be and ^{231}Pa, *Earth Planet. Sci. Lett.*, *96*, 287–304, doi:10.1016/0012-821X(90)90008-L.

Bacon, M. P. (1984), Glacial to interglacial changes in carbonate and clay sedimentation

in the Atlantic-Ocean estimated from Th-230 measurements, *Isot. Geosci.*, 2(2), 97–111.

Bacon, M. P., and R. F. Anderson (1982), Distribution of thorium isotopes between dissolved and particulate forms in the deep sea, *J. Geophys. Res.*, 87, 2045–2056, doi:10.1029/JC087iC03p02045.

Bacon, M. P., D. W. Spencer, and P. G. Brewer (1976), ^{210}Pb/^{226}Ra and ^{210}Po/^{210}Pb disequilibria in seawater and suspended particulate matter, *Earth Planet. Sci. Lett.*, 32, 277–296, doi:10.1016/0012-821X(76)90068-6.

Berelson, W. M., et al. (1997), Biogenic budgets of particle rain, benthic remineralization, and sediment accumulation in the equatorial Pacific, *Deep Sea Res., Part II*, 44, 2251–2282, doi:10.1016/S0967-0645(97)00030-1.

Broecker, W., S. Barker, E. Clark, I. Hajdas, and G. Bonani (2006), Anomalous radiocarbon ages for foraminifera shells, *Paleoceanography*, 21, PA2008, doi:10.1029/2005PA001212.

Chase, Z., R. F. Anderson, M. Q. Fleisher, and P. W. Kubik (2002), The influence of particle composition and particle flux on scavenging of Th, Pa and Be in the ocean, *Earth Planet. Sci. Lett.*, 204, 215–219, doi:10.1016/S0012-821X(02)00984-6.

Chen, J. H., R. L. Edwards, and G. J. Wasserburg (1986), ^{238}U, ^{234}U and ^{232}Th in seawater, *Earth Planet. Sci. Lett.*, 80, 241–251, doi:10.1016/0012-821X(86)90108-1.

Edwards, N. R., and R. Marsh (2005), Uncertainties due to transport-parameter sensitivity in an efficient 3-D ocean-climate model, *Clim. Dyn.*, 24(4), 415–433, doi:10.1007/s00382-004-0508-8.

Francois, R., M. Frank, M. M. Rutgers van der Loeff, and M. P. Bacon (2004), ^{230}Th normalization: An essential tool for interpreting sedimentary fluxes during the late Quaternary, *Paleoceanography*, 19, PA1018, doi:10.1029/2003PA000939.

Francois, R., et al. (2007), Comment on "Do geochemical estimates of sediment focusing pass the sediment test in the equatorial Pacific?" by M. Lyle et al. (2005), *Paleoceanography*, 22, PA1216, doi:10.1029/2005PA001235.

Frank, M., J.-D. Eckhardt, A. Eisenhauer, P. W. Kubik, B. Dittrich-Hannen, M. Segl, and A. Mangini (1994), Beryllium 10, thorium 230 and protactinium 231 in Galapagos microplate sediments: Implications of hydrothermal activity and paleoproductivity changes during the last 100,000 years, *Paleoceanography*, 9, 559–578, doi:10.1029/94PA01132.

Franzese, A. M., S. R. Hemming, S. L. Goldstein, and R. F. Anderson (2006), Reduced Agulhas leakage during the Last Glacial Maximum inferred from an integrated provenance and flux study, *Earth Planet. Sci. Lett.*, 250, 72–88, doi:10.1016/j.epsl.2006.07.002.

Geibert, W., and R. Usbeck (2004), Adsorption of thorium and protactinium onto different particle types: Experimental findings, *Geochim. Cosmochim. Acta*, 68(7), 1489–1501, doi:10.1016/j.gca.2003.10.011.

Griffies, S. M. (1998), The Gent-McWilliams skew flux, *J. Phys. Oceanogr.*, 28, 831–841.

Henderson, G. M., and R. F. Anderson (2003), The U-series toolbox for paleoceanography, *Rev. Mineral. Geochem.*, 52, 493–531, doi:10.2113/0520493.

Henderson, G. M., C. Heinze, R. F. Anderson, and A. M. E. Winguth (1999), Global distribution of the ^{230}Th flux to ocean sediments constrained by GCM modelling, *Deep Sea Res., Part I*, 46, 1861–1894, doi:10.1016/S0967-0637(99)00030-8.

Honeyman, B. D., L. S. Balistrieri, and J. W. Murray (1988), Oceanic trace metal scavenging: The importance of particle concentration, *Deep Sea Res., Part A*, 35, 227–246, doi:10.1016/0198-0149(88)90038-6.

Khatiwala, S., M. Visbeck, and M. A. Cane (2005), Accelerated simulation of passive tracers in ocean circulation models, *Ocean Model.*, 9, 51–69.

Kienast, S. S., M. Kienast, A. C. Mix, S. E. Calvert, and R. François (2007), Thorium-230 normalized particle flux and sediment focusing in the Panama Basin region during the last 30,000 years, *Paleoceanography*, 22, PA2213, doi:10.1029/2006PA001357.

Kumar, N. (1994), Trace metals and natural radionuclides as tracers of ocean productivity, Ph.D. thesis, 317 pp., Columbia Univ., New York.

Lao, Y., R. F. Anderson, W. S. Broecker, S. E. Trumbore, H. J. Hofmann, and W. Wolfli (1992), Transport and burial rates of ^{10}Be and ^{231}Pa in the Pacific Ocean during the Holocene period, *Earth Planet. Sci. Lett.*, 113, 173–189, doi:10.1016/0012-821X(92)90218-K.

Li, Y.-H. (2005), Controversy over the relationship between major components of sediment-trap materials and the bulk distribution coefficients of ^{230}Th, ^{231}Pa and ^{10}Be, *Earth Planet. Sci. Lett.*, 233, 1–7, doi:10.1016/j.epsl.2005.02.023.

Loubere, P., F. Mekik, R. Francois, and S. Pichat (2004), Export fluxes of calcite in the eastern equatorial Pacific from the Last Glacial Maximum to present, *Paleoceanography*, 19, PA2018, doi:10.1029/2003PA000986.

Luo, S., and T.-L. Ku (1999), Oceanic ^{231}Pa/^{230}Th ratio influenced by particle composition and remineralisation, *Earth Planet. Sci. Lett.*, 167, 183–199, doi:10.1016/S0012-821X(99)00035-7.

Luo, S., and T.-L. Ku (2004a), On the importance of opal, carbonate, and lithogenic clays in scavenging and fractionating ^{230}Th, ^{231}Pa and ^{10}Be in the ocean, *Earth Planet. Sci. Lett.*, 220, 201–211, doi:10.1016/S0012-821X(04)00027-5.

Luo, S., and T.-L. Ku (2004b), Reply to comment on "On the importance of opal, carbonate, and lithogenic clays in scavenging and fractionating ^{230}Th, ^{231}Pa and ^{10}Be in the ocean," *Earth Planet. Sci. Lett.*, 220, 223–229, doi:10.1016/S0012-821X(04)00029-9.

Lyle, M., A. Mix, and N. Pisias (2002), Patterns of CaCO$_3$ deposition in the eastern tropical Pacific Ocean for the last 150 kyr: Evidence for a southeast Pacific depositional spike during marine isotope stage (MIS) 2, *Paleoceanography*, 17(2), 1013, doi:10.1029/2000PA000538.

Lyle, M., N. Mitchell, N. Pisias, A. Mix, J. I. Martinez, and A. Paytan (2005), Do geochemical estimates of sediment focusing pass the sediment test in the equatorial Pacific?, *Paleoceanography*, 20, PA1005, doi:10.1029/2004PA001019.

Marcantonio, F., N. Kumar, M. Stute, R. F. Anderson, M. A. Seidl, P. Schlosser, and A. Mix (1995), Express letter: A comparative study of accumulation rates derived by He and Th isotope analysis of marine sediments, *Earth Planet. Sci. Lett.*, 133, 549–555, doi:10.1016/0012-821X(95)00079-R.

Marcantonio, F., R. F. Anderson, M. Stute, N. Kumar, P. Schlosser, and A. Mix (1996), Extraterrestrial ^{3}He as a tracer of marine sediment transport and accumulation, *Nature*, 383, 705–707, doi:10.1038/383705a0.

Marcantonio, F., R. F. Anderson, S. Higgins, M. Stute, P. Schlosser, and P. Kubik (2001), Sediment focusing in the central equatorial Pacific Ocean, *Paleoceanography*, 16, 260–267, doi:10.1029/2000PA000540.

Marchal, O., R. Francois, T. F. Stocker, and F. Joos (2000), Ocean thermohaline circulation and sedimentary ^{231}Pa/^{230}Th ratio, *Paleoceanography*, 15, 625–641, doi:10.1029/2000PA000496.

McGee, D., F. Marcantonio, and J. Lynch-Stieglitz (2007), Deglacial changes in dust flux in the eastern equatorial Pacific, *Earth Planet. Sci. Lett.*, 257, 215–230, doi:10.1016/j.epsl.2007.02.033.

Mollenhauer, G., J. F. McManus, A. Benthien, P. J. Müller, and T. I. Eglinton (2006), Rapid lateral particle transport in the Argentine Basin: Molecular ^{14}C and ^{230}Th$_{xs}$ evidence, *Deep Sea Res., Part I*, 53, 1224–1243, doi:10.1016/j.dsr.2006.05.005.

Moore, W. S. (1981), The thorium isotope content of ocean water, *Earth Planet. Sci. Lett.*, 53, 419–426, doi:10.1016/0012-821X(81)90046-7.

Müller, S. A., F. Joos, N. R. Edwards, and T. F. Stocker (2006), Water mass distribution and ventilation time scales in a cost-efficient, 3-dimensional ocean model, *J. Clim.*, 19, 5479–5499, doi:10.1175/JCLI3911.1.

Nozaki, Y., and T. Nakanishi (1985), Pa-231 and Th-230 profiles in the open ocean water column, *Deep Sea Res., Part A*, 32, 1209–1220.

Nozaki, Y., S. H. Yang, and M. Yamada (1987), Scavenging of thorium in the ocean, *J. Geophys. Res.*, 92, 772–778, doi:10.1029/JC092iC01p00772.

Pichat, S., K. W. W. Sims, R. François, J. F. McManus, S. Brown Leger, and F. Albarède (2004), Lower export production during glacial periods in the equatorial Pacific derived from (^{231}Pa/^{230}Th)$_{xs,0}$ measurements in deep-sea sediments, *Paleoceanography*, 19, PA4023, doi:10.1029/2003PA000994.

Roy-Barman, M., J. H. Chen, and G. J. Wasserburg (1996), ^{230}Th-^{232}Th systematics in the central Pacific Ocean: The sources and fates of thorium, *Earth Planet. Sci. Lett.*, 139, 351–363, doi:10.1016/0012-821X(96)00017-9.

Siddall, M., G. M. Henderson, N. R. Edwards, S. A. Müller, T. F. Stocker, F. Joos, and M. Frank (2005), ^{231}Pa/^{230}Th fractionation by ocean transport, biogenic particle flux and particle type, *Earth Planet. Sci. Lett.*, 237, 135–155, doi:10.1016/j.epsl.2005.03.031.

Siddall, M., T. F. Stocker, R. Spahni, T. Blunier, J. F. McManus, and E. Bard (2006), Using a maximum simplicity model to simulate millennial variability during the last four glacial periods, *Quat. Sci. Rev.*, 25, 3185–3197, doi:10.1016/j.quascirev.2005.12.014.

Siddall, M., T. F. Stocker, G. M. Henderson, F. Joos, M. Frank, N. R. Edwards, S. P. Ritz, and S. A. Müller (2007), Modeling the relationship between ^{231}Pa/^{230}Th distribution in North Atlantic sediment and Atlantic meridional overturning circulation, *Paleoceanography*, 22, PA2214, doi:10.1029/2006PA001358.

Skinner, L. C., and N. J. Shackleton (2005), An Atlantic lead over Pacific deep-water change across Termination I: Implications for the application of the marine isotope stage stratigraphy, *Quat. Sci. Rev.*, 24, 571–580, doi:10.1016/j.quascirev.2004.11.008.

Thomas, E., K. K. Turekian, and K. Y. Wei (2000), Productivity control of fine particle transport to equatorial Pacific sediment,

Global Biogeochem. Cycles, *14*(3), 945–955, doi:10.1029/1998GB001102.

Yang, Y.-L., H. Elderfield, and M. Ivanovich (1990), Glacial to Holocene changes in carbonate and clay sedimentation in the equatorial Pacific Ocean estimated from thorium 230 profiles, *Paleoceanography*, *5*, 789–809, doi:10.1029/PA005i005p00789.

Yu, E. F., R. Francois, and M. P. Bacon (1996), Similar rates of modern and last-glacial ocean thermohaline circulation inferred from radiochemical data, *Nature*, *379*, 689–694, doi:10.1038/379689a0.

————————————

R. F. Anderson, L. I. Bradtmiller, A. Franzese, D. McGee, M. Siddall, and G. Winckler, Lamont-Doherty Earth Observatory of Columbia University, 61 Route 9W, Palisades, NY 10964, USA. (siddall@ldeo.columbia.edu)

G. M. Henderson, Department of Earth Sciences, Oxford University, Parks Road, OX1 3PR Oxford, UK.

S. A. Müller, Department of Earth and Environmental Sciences, Open University, MK7 6AA Milton Keynes, UK.

T. F. Stocker, Climate and Environmental Physics, Physics Institute, University of Bern, CH-3012 Bern, Switzerland.